Available online at www.sciencedirect.com
ScienceDirect
Journal of Magnetic Resonance 187 (2007) 251–257
JMR Journal of Magnetic Resonance
www.elsevier.com/locate/jmr

Measurement of multilamellar onion dimensions under shear using frequency domain pulsed gradient NMR

Antoine Lutti, Paul T. Callaghan *

MacDiarmid Institute for Advanced Materials and Nanotechnology, School of Chemical and Physical Sciences, Victoria University of Wellington, New Zealand

Received 19 March 2007; revised 3 May 2007
Available online 22 May 2007

Abstract

We present a simple method by which the dimensions of shear-induced multilamellar vesicles (MLVs), also known as onions, can be measured during the shearing process itself. This approach is based on the use of a closely spaced train of magnetic field gradient pulses applied during a CPMG echo sequence. The CPMG train compensates flow effects while the frequency-dependence of apparent diffusion can reveal the onion size. We present here a simple phenomenological model for restricted diffusion in multilamellar vesicles, which may be used to interpret the resulting diffusion spectrum. We demonstrate this approach with MLVs formed from the lamellar phase of sodium dodecyl sulfate (SDS) in water and octanol.

Keywords: Diffusion; Bilayers; Liquid crystals; Onion; Shear; rheo-NMR; Lamellae

1. Introduction

Lamellar surfactant systems are planar aggregates of amphiphilic molecules separated by layers of solvent [1–3]. Here, we are concerned with lyotropic systems, where topological characteristics of the phase are determined by the relative amount of each species present in the system. Ideally, a lamellar system forms a highly ordered smectic phase, with a well-defined lamellar spacing. The presence of defects on the membranes and distributions of angular orientations of the lamellae are deviations from the ideal case that are frequently observed in practical situations [4,5]. For ionic surfactant systems, dilution of electrolytes into the solvent reduces interlamellar electrostatic interactions [6]. Helfrich interactions, arising from steric collisions between neighboring membranes, are then dominant [7–9]. In this paper, we are particularly interested in the effect of shear on lamellar systems. The smectic distance of a Helfrich stabilised system is a solid-like property of the phase. Its preservation drives lamellar reaction to a perturbation and the behaviour of a well-aligned smectic system in a flow field is strongly dependent upon the direction of the deformation with respect to the orientation of the bilayers [4]. It has been shown that at low deformation rates, shear flow may induce lamellar orientation [11–13], most commonly with lamellae directors oriented along the velocity gradient direction (parallel direction or so-called (“c-orientation”). Shear may also damp bilayer fluctuations [14]. Furthermore, evidence from light scattering studies suggests that shear can reduce defects in the lamellar structure [4,10].

If the shear rate is sufficiently high, spherical vesicles may be formed by shear-induced buckling of the membranes [16]. Onion formation has been confirmed experimentally using various techniques and chemical systems [17–21]. The newly formed multilamellar vesicles (MLV) have proved to remain stable over several days after ceasing shear [21]. However, it is of some interest to use experimental methods which are capable of determining onion dimensions during the shearing process itself, so that formation processes may be studied.

* Corresponding author. Fax: +64 650 5164.
E-mail address: Paul.Callaghan@vuw.ac.nz (P.T. Callaghan).

1090-7807/$ - see front matter © 2007 Elsevier Inc. All rights reserved.
doi:10.1016/j.jmr.2007.05.003

The object of the present paper is to demonstrate a new NMR method for the measurement of multilamellar vesicle dimensions under shear. Our approach is based on the use of multiple pulses of magnetic field gradients inserted in a Carr-Purcell-Meiboom-Gill echo train, whose refocusing properties remove dephasing effects due to inhomogeneous flow, but retain the incoherent dephasing associated with molecular diffusion [22–24]. This diffusion of water, being confined to onion bilayers, is strongly restricted and has a time-dependence of mean-squared displacement which depends upon onion size. In our multiple gradient pulse CPMG method, the natural domain of description is the frequency domain of the velocity autocorrelation function (the so-called diffusion spectrum). This method has been extensively discussed by Stepisnik [26], and demonstrated by Callaghan and Stepisnik, and numerous subsequent studies [27–31]. In this paper, we describe a simple phenomenological model for restricted diffusion and derive formula for the diffusion spectrum and its dependence on onion size. We present here NMR evidence for onion formation in the lamellar phase of SDS/water induced by shear applied via a Couette Cell located in the NMR spectrometer. The fluid phase is located between two concentric cylindrical tubes of 16 mm (OD) and 18 mm (ID), the inner cylinder being rotated at a frequency tuned by the experimenter (strain-controlled experiment). In Section 2, we illustrate onion formation using NMR deuterium spectroscopy, while in Section 3, we focus on the restricted diffusion of solvent molecules embedded within the lamellae.

2. Experimental evidence for onion formation

In the present study, the chemical system is a mixture of sodium dodecyl sulfate (SDS) surfactant molecules and octanol diluted in brine. The respective concentration of each species is 6.5 wt% SDS, 7.8 wt% octanol, 85.7 wt% brine at 20 g L^{-1}. For those mass ratios, a lamellar phase of soft bilayers is formed [32], where the layer spacing is $d = 15$ nm and the layer thickness $\delta = 2$ nm [19,20]. Fig. 1 shows the evolution of the D_2O NMR spectrum as shear is increased. This was obtained by replacing water molecules H_2O) by heavy water molecules (D_2O). We are sufficiently far from phase boundary that this replacement is not expected to affect the lamellar phase. The NMR experiments were carried out at 7 T field strength. The splitting of the spectrum at low shear rates, reflecting ordering of the initial lamellar phase, gradually disappears. At $\dot{\gamma} = 1.5\ s^{-1}$, it is replaced by a unique peak, suggesting probing by the D_2O molecules of all possible orientations with respect to the polarising magnetic field $\mathbf{B}_0$. This is a clear indication of the formation of approximately isotropic vesicles at this shear rate [12,13]. This is may provide an indication of the formation of approximately isotropic vesicles at this shear rate [12,13] although, it is also possible that these changes of the deuterium spectrum under shear reflect destruction of the bilayers. As we shall show in the diffusion measurements performed here, the former explanation is more likely to be correct.

We now turn our attention to the diffusion of solvent molecules embedded within the shear-induced structures. In the measurements presented here, signal arises from a volume of sample within the Couette Cell where solvent diffusion along the directions $\vec{\nabla}\vec{v}$, $\vec{v}$, respectively radial and tangential to the Couette Cell, and the direction $\vec{\nabla} \times \vec{v}$ aligned along the main axis of the Couette Cell, can be accessed separately (see Fig. 2a). Note that in hydrodynamic language $\vec{\nabla}\vec{v}$ is the gradient of flow direction, $\vec{v}$ is the flow direction and $\vec{\nabla} \times \vec{v}$ is the vorticity direction.

The corresponding results, displayed in Fig. 2b), confirm the formation of near spherical vesicles: diffusion becomes closer to isotropic as shear is increased. However, diffusion

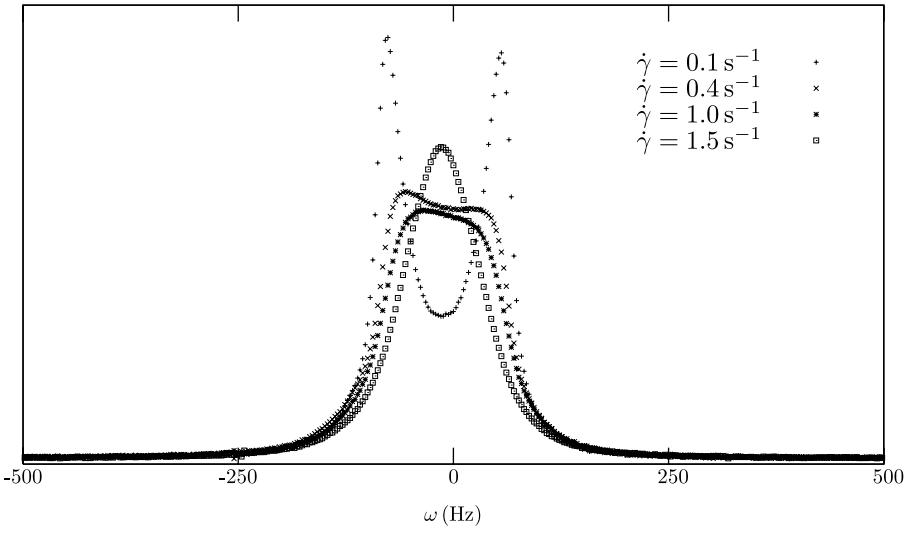

Fig. 1. D_2O NMR spectra of a lamellar phase subjected to various shear rates: splitting of the spectrum at $\dot{\gamma} = 1.5\ s^{-1}$, reflecting ordering of the lamellar system at this shear rate, is gradually replaced by a unique peak as the applied shear rate is increased. This evolution is typical of the transition from a lamellar to an isotropic phase.

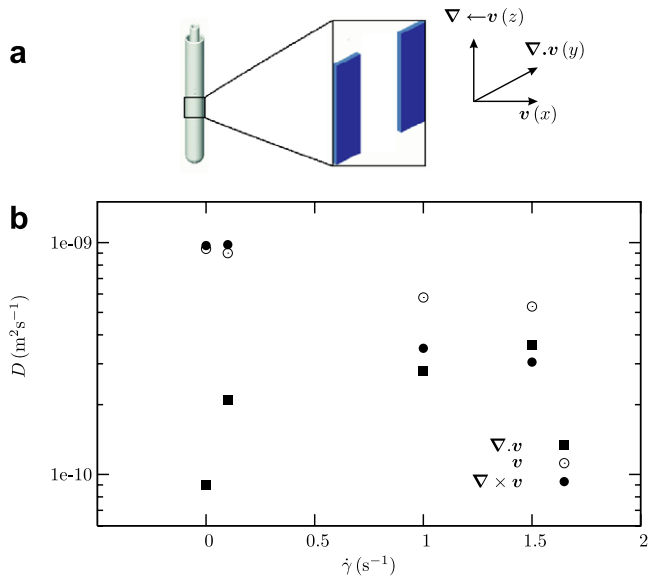

Fig. 2. Anisotropic diffusion coefficients for various applied shear rates: in those experiments, signal arises from a volume of sample where diffusion along the gradient-of-flow ($\vec{\nabla}.\vec{v}$), flow ($\vec{v}$) and vorticity ($\vec{\nabla} \times \vec{v}$) directions can be distinguished (a). The cartesian axes assigned to each direction are also shown. As $\dot{\gamma}$ is increased, diffusion coefficients along those three directions tend towards a common value, confirming the formation of near-isotropic vesicles (b).

remains faster along the flow direction as the vesicles are formed $\dot{\gamma} = 1.5\ \mathrm{s^{-1}}$. This will be treated in more detail in Section 4, where we relate solvent diffusion to the shape of the onions.

Note that the details of shear-dependent rheology and shear-dependent onion size will be discussed in a subsequent paper. Here we develop the diffusion spectrum model and prove its application to onion size measurement in Section 4.

3. Diffusion spectrum of an onion phase

The idea behind the diffusion spectrum as measured by multiple gradient pulse CPMG techniques has been discussed in detail in earlier papers [26–31]. The crucial theoretical tool in calculating the diffusion spectrum is the velocity autocorrelation function (VACF). Hence, all description of the diffusion dynamics must be cast in these terms. Furthermore, since the diffusion spectrum is the Fourier transform of the VACF, we must have knowledge of the VACF from zero time out to infinite time. In consequence, all transitions in the restricted motion of the molecular diffusion under study must be represented in the hierarchy of timescales. In what follows we build up, step by step, a description of the diffusive process from the shortest to longest times.

3.1. Time-dependence of the solvent diffusion coefficient

We begin by setting up a coordinate system for the description of diffusion in an MLV onion. The Fig. 3 shows the relevant geometry, in (a) the multi-bilayer structure, with (b) a chosen shell of radius r in which a local section of water layer is shown. We choose to describe diffusion coefficients respectively perpendicular and parallel to the bilayer normals as $D_\perp(t)$ and $D_\parallel(t)$. The spherical polar coordinate geometry is shown in (c). In the NMR experiment the magnetic field gradient, used to encode for motion, is applied along some pre-determined axis. We will label this axis z for simplicity. The quantity measurable in NMR, $D_{\alpha\alpha}$, is the local projection of $D_\perp(t)$ and $D_\parallel(t)$ along that α direction (see Fig. 3). We here focus on a small segment of fluid layer in the radius r shell at polar and azimuthal angle coordinates (Θ, Φ) and in order to correspond with Fig. 3 we set α to be z. Then for diffusion along z the displacements are azimuth independent and given by:

$$D_{zz}(t,\Theta) = D_\perp(t)\cos^2\Theta(t) + D_\parallel(t)\sin^2\Theta(t) \tag{1}$$

For spherical multi lamellar vesicles, the three directions of the cartesian system are equivalent. We will find experimentally however that under shear flow conditions, distortion is observed, as indicated by differing diffusive

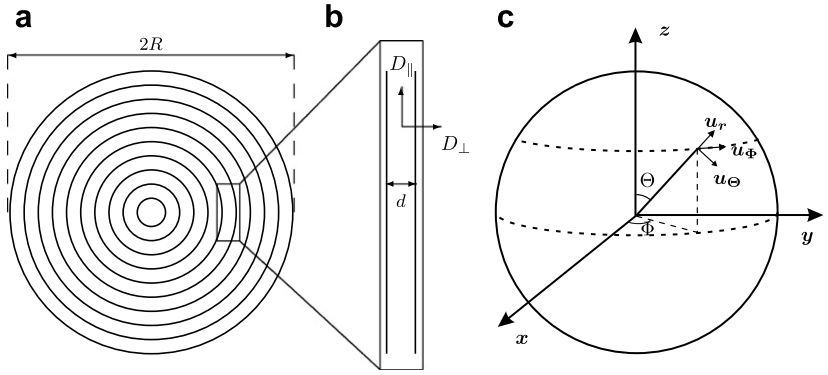

Fig. 3. A Multilamellar Vesicle (a): the interlayer spacing value $d \approx 10^{-8}$ m leads to a typical decay time for diffusion perpendicular to the membranes $\tau_c \sim 10^{-8}$ s too short to be accessible by our sequence (b). The much higher onion size $R \sim 10^{-6}$ m leads diffusion parallel to the membranes to decay over a time$\tau_d \sim 10^{-3}$ s. For simplicity, we describe motions along the z-direction, where the displacements are azimuth independent (c).

behaviour when the α axis is selected to lie along the flow, flow-gradient or vorticity directions.

In order to derive the velocity autocorrelation function at all times, we attempt to write down the observation time-dependent diffusion coefficient, since we will use the result,

$$\langle v_\alpha(t)v_\alpha(0)\rangle = \frac{\partial\langle D_{\alpha\alpha}(t)\rangle}{\partial t} \tag{2}$$

We begin at the shortest time, much shorter than the time τ_c for molecules to diffuse the water thickness d. Few water molecules will have a chance to collide with the bilayer, and so $D_\perp(t)$ and $D_\parallel(t)$ reduce to the free diffusion coefficient D of the solvent. However, as time passes, an increasing number of molecules encounter the bilayers in their displacements perpendicular to the membranes. To encompass this behaviour we write:

$$D_\perp(t) = D_{\text{perm}} + (D - D_{\text{perm}})\mathrm{e}^{-\frac{t}{\tau_c}} \tag{3}$$

where the decay time $\tau_c \approx \frac{d^2}{2D}$ of $D_\perp(t)$ is the time required by the water molecule spins to travel over one interlayer distance. D_{perm} is the permeation coefficient of the water molecules through the various defects present on the membranes. Note that Eq. (3) is phenomenological. It expresses the correct limiting cases as $t \ll \tau_c$ and $t \gg \tau_c$. The details of the crossover may not be exact, but the essential physics is represented in terms of a mathematical function which is easily handled in subsequent analytic manipulations. This simple device we shall follow in the higher time scale hierarchies as well.

Of course the NMR experiment has contributions from all segments (Θ,Φ) within a shell of radius r, as well as from all shell radii. Consider first the case of a shell of particular radius. Provided that diffusion distances are sufficiently short so that a unique Θ can be ascribed to each water molecule we may write:

$$\begin{aligned}\langle D_{\alpha\alpha}(t)\rangle &= \frac{\int_0^\pi D_{\alpha\alpha}(t,\Theta)P(\Theta)\,\mathrm{d}\Theta}{\int_0^\pi P(\Theta)\,\mathrm{d}\Theta}\\ &= \frac{\int_0^\pi (D_\perp(t)\cos^2\Theta + D_{||}(t)\sin^2\Theta)\sin\Theta\,\mathrm{d}\Theta}{\int_0^\pi \sin\Theta\,\mathrm{d}\Theta}\\ &= \frac{D_\perp(t) + 2D_{||}(t)}{3}\end{aligned} \tag{4}$$

where $P(\Theta) = \sin\Theta$ is the polar angle distribution. Suppose instead we allow for longer times, such that water molecules explore differing (Θ,Φ) coordinates. An exact expression for $D_{\alpha\alpha}(t)$ taking the diffusion of molecules over ranges of (Θ,Φ) is possible, but we prefer simpler device, namely to write a simpler analytic expression which correctly contains the limits and the physics of the crossover. The characteristic crossover time is now $\tau_d \approx \frac{r^2}{2D}$. Consider first the short time behavior $t \ll \tau_d$. In this case, combining Eqs. (4) and (3), allowing $D_\parallel(t) = D$, we have:

$$\langle D_{\alpha\alpha}(t)\rangle = \frac{D_{\text{perm}} + (D - D_{\text{perm}})\mathrm{e}^{-\frac{t}{\tau_c}} + 2D}{3} \tag{5}$$

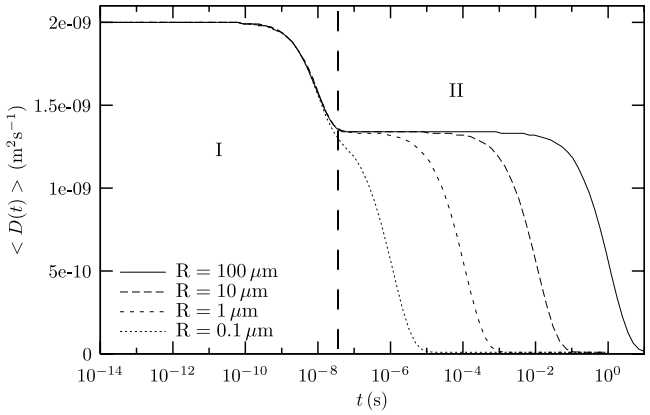

Fig. 4. Time-dependence of solvent molecules diffusion coefficient: the first decrease is due to decay of $D_\perp(t)$towards D_{perm} (Eq. (3)) and occurs over a time scale too short to be observable with our technique. The second decay occurs at a time scale observable experimentally. Here, D and D_{perm} are respectively set to 2×10^{-9} and 3×10^{-11} $\mathrm{m^2\,s^{-1}}$ arbitrarily.

In the long time case, consider first the long time behavior $t \gg \tau_d$, $D_{\alpha\alpha}(t)$ must reach the limiting case of D_{perm}, since only permeation through the bilayers can permit diffusion on a greater distance than r. For convenience we can assign this timescale as $\tau_d \approx \frac{r^2}{2D}$. Following the phenomenological approach of Eq. (3) an expression which encompasses both limits is:

$$\langle D_{\alpha\alpha}(t)\rangle = D_{\text{perm}} + (D - D_{\text{perm}})\frac{\mathrm{e}^{-\frac{t}{\tau_c}} + 2\mathrm{e}^{-\frac{t}{\tau_d}}}{3} \tag{6}$$

The time-dependence of $\langle D_{\alpha\alpha}(t)\rangle$ is illustrated in Fig. 4, with the ordinate written $D(t)$ since for spherical onions no axis distinction need be made. Here, we are concerned with water molecules $D \approx 2.3\times10^{-9}\,\mathrm{m^2\,s^{-1}}$ diffusing between bilayers separated by a distance $d \sim 10^{-8}$ m (see Fig. 3) leading to: $\tau_c \sim 10^{-8}$ s, much shorter than any timescale accessible with our NMR-diffusion sequence ($\sim 10^{-3}$ s). Solvent collision with the membranes on their trajectories perpendicular to the bilayers is therefore not observable experimentally. However, a typical value for the onion layer radius is $r \sim 10^{-6}$ m, leading to: $\tau_d \sim 10^{-3}$ s. Decay of solvent diffusion parallel to the membranes occurs on a timescale accessible by NMR-diffusion techniques and may therefore be observable.

Finally our analysis requires that we average our expression over all shell diameters r up to the onion size R. Onions consist of concentric spherically-shaped bilayers and separated by a distance $d \sim 10$ nm. In practical terms, the sphere radius therefore ranges from the nanometer scale up to the onion outer radius $R \sim \mu$m. Note that for $D_{\text{perm}} \ll D$, we might naively expect water molecules trapped within a shell of radius r to explore the full shell dimensions before migration through a bilayer to a neighboring shell. However the ratio of the time taken for inter-bilayer collisions to that for diffusion around the sphere is on the order of $\frac{d^2}{r^2} \sim 10^{-4}$. In practice we find $D_{\text{perm}} \sim 10^{-2}D$ so that we might expect significant bilayer

permeation. However permeation merely translates the water molecule location from a shell of radius r to one of radius $r+d$ or $r-d$, and given $d \ll r$, no significant change to the diffusion behaviour which is characterised by the correlation time $\tau_d(r)$. Hence, it is reasonable to assert that a given local value of $\tau_d(r)$ prevails in the entire azimuthal exploration of the onion. That means we must average NMR signals acquired from layers with different $\tau_d(r)$ values rather than average $\tau_d(r)$ itself across the distribution of layers. We thus obtain an expression based on our calculation of the diffusion spectrum for a single shell, making radial averaging the final step.

3.2. Onions and the diffusion spectrum

The velocity autocorrelation function of the solvent molecules at times t much greater than the solvent molecule collision time τ_0 is [31]:

$$\begin{aligned}\langle v_\alpha(t)v_\alpha(0)\rangle &= \frac{\partial\langle D_{\alpha\alpha}(t)\rangle}{\partial t} \\ &= -\frac{(D-D_{\text{perm}})}{3}\left(\frac{1}{\tau_c}e^{-\frac{t}{\tau_c}}+\frac{2}{\tau_d}e^{-\frac{t}{\tau_d}}\right)\end{aligned}$$

In order to correctly differentiate and then obtain the Fourier spectrum, we must also account for the region in the vicinity of the time origin where intermolecular collisions prevail. Here $\langle v_\alpha(t)v_\alpha(0)\rangle = \frac{D}{\tau_0}e^{-\frac{t}{\tau_0}}$. Accounting for this contribution to the diffusion spectrum, the quantity measurable in NMR ($t \gg \tau_0$) is:

$$\begin{aligned}D_{\alpha\alpha}(\omega) &= \int_0^\pi \langle v_\alpha(t)v_\alpha(0)\rangle e^{i\omega t}dt \\ &= D-\frac{D-D_{\text{perm}}}{3}\left[\frac{1}{1+(\omega\tau_c)^2}+\frac{2}{1+(\omega\tau_d)^2}\right] \qquad (7)\end{aligned}$$

As $\tau_d(r)$ so $D_{\alpha\alpha}(\omega)$ is a function of radius r. Eq. (7) requires averaging over the local layer radius within the multilamellar vesicle. An interesting question arises as to the lower limit. It could be argued that there will be a maximum curvature possible that may imply a lower limit to the radii and lead to a finite sized inner water-filled core. We might estimate this limiting inner radius to be much smaller than the outer dimensions of the onion, perhaps even on the order of the lamellar separation d, but certainly sufficiently small that the volume contribution is very small, and, on the experimental timescale the diffusion of water in this inner core is restricted by the surrounding lamellae and so little distinguished from interlamellar water. Setting the lower limit radius as zero,

$$\langle D_{\alpha\alpha}(\omega)\rangle = \int_0^R D_{\alpha\alpha}(\omega)P(r)dr$$

Where $P(r) = \frac{4\pi r^2}{\frac{4}{3}\pi R^3}$ is the probability density for a solvent molecule to be located between r and $r+dr$. We get:

$$\begin{aligned}\langle D_{\alpha\alpha}(\omega)\rangle = D &- \frac{D-D_{\text{perm}}}{3}\frac{1}{1+(\omega\tau_c)^2} \\ &- (D-D_{\text{perm}})\left(\frac{1}{R}\sqrt{\frac{D}{\omega}}\right)^3 * \left\{-2\tan^{-1}\left(1-R\sqrt{\frac{\omega}{D}}\right)\right. \\ &+2\tan^{-1}\left(1+R\sqrt{\frac{\omega}{D}}\right)+\ln\left(\frac{2D}{\omega}-2R\sqrt{\frac{D}{\omega}}+R^2\right) \\ &\left.-\ln\left(\frac{2D}{\omega}+2R\sqrt{\frac{D}{\omega}}+R^2\right)\right\} \qquad (8)\end{aligned}$$

Note that the analytic form of Eq. (8) is a consequence of the simple exponential correlation function assumptions in our model. We make no claim that Eq. (8) is precise, although its closed form does make the fitting of diffusion spectra data much easier. Note further that a lack of knowledge of the details of the region I to region II crossover at $\omega\tau_c \sim 1$, does not affect the accuracy of the region II from of the expression. In other words the form of $D(\omega)$ is independent of τ_c when $\omega\tau_c \ll 1$.

An illustration of the diffusion spectra of solvent molecules diffusing within MLVs is shown in Fig. 5 for different onion radii R. The effect of onion size R is clear and follows our expectations: the decay of $D_{\alpha\alpha}(\omega)$ towards D_{perm} occurs at higher frequencies (i.e. shorter times) as the onion size is reduced. In the following, we test the relevance of our phenomenological model on diffusion spectra obtained experimentally. The onion radius R is a free parameter used for the fitting of the data.

4. Experimental: measurement of onion size under shear

Here, experimental diffusion spectrum data are presented for the sodium dodecyl sulfate (SDS) surfactant system (see Section 2). The pulse sequence used is shown in Fig. 6, and further details concerning its use, as well as the resilience of the method to shear flow, can be found in reference [15]. According to the diffusion spectrum for-

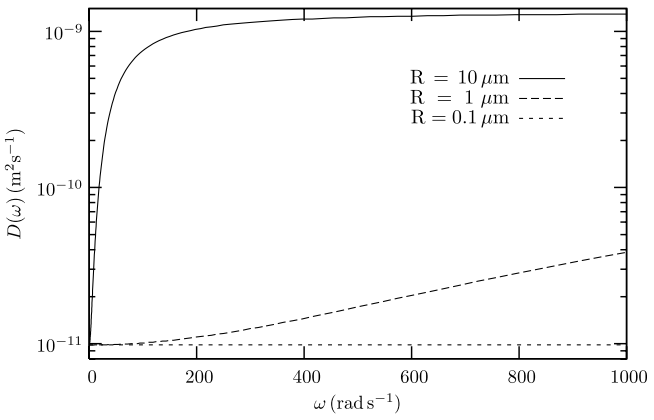

Fig. 5. An illustration of the diffusion spectrum for an onion phase, obtained using numerical methods: the effect of the onion size is clearly visible: the bigger the onion the lower the frequencies (the longer the time) required for solvent diffusion to decay to the permeation value.

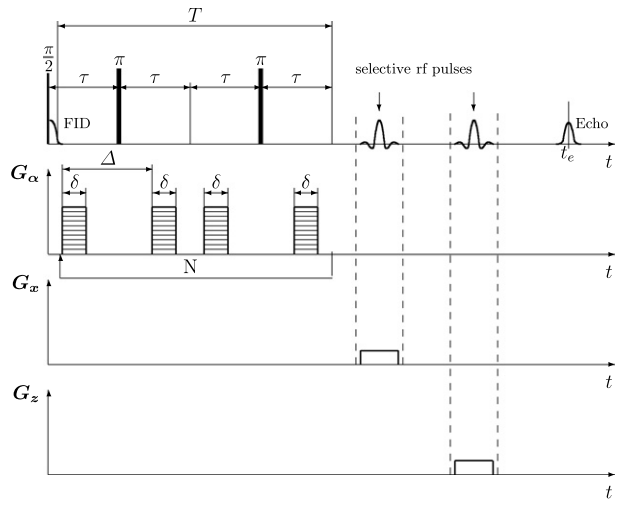

Fig. 6. Multi Pulsed Gradient Spin Echo experiment: the repetitive train of repeated four diffusion-encoding gradient pulses enables for the measurement of diffusion while compensating for flow artifact (for further details see [15]). The diffusion-encoding gradient, G_α, may be applied along any of the Cartesian axes. It is followed by slice selective rf/gradient pulse combinations enabling for the selection of a volume of sample where diffusion along the $\vec{\nabla}\vec{v}$, $\vec{v}$ and $\vec{\nabla}\times\vec{v}$ directions can be distinguished (Fig. 2a). δ is in the range 1–3 ms. The slice thickness are 1 mm normal to x and 30 mm normal to z.

malism developed by Callaghan and Stepisnik, motion is encoded over a duration T, the observation time of the NMR sequence [31,32]. The measurement is repeated for different values of T and the measured diffusion coefficients are plotted versus a frequency $\omega = \frac{2\pi}{T}$. The resulting diffusion spectrum $D_{\alpha\alpha}(\omega)$ of the solvent molecules may display features typical of the lamellar phase under study [14].

For the data presented here: 8 ms $\leqslant T \leqslant$ 200 ms, leading to: 31 $s^{-1} \leqslant \omega \leqslant$ 785 s^{-1}. The applied shear rate is $\dot{\gamma} = 1.5\ s^{-1}$, for which D_2O spectroscopy indicates that isotropic structures are formed (see Fig. 1). Shear was applied for 1.5 h prior to the start of the experiments. Previous tests have proved that flow artifacts are negligible under those

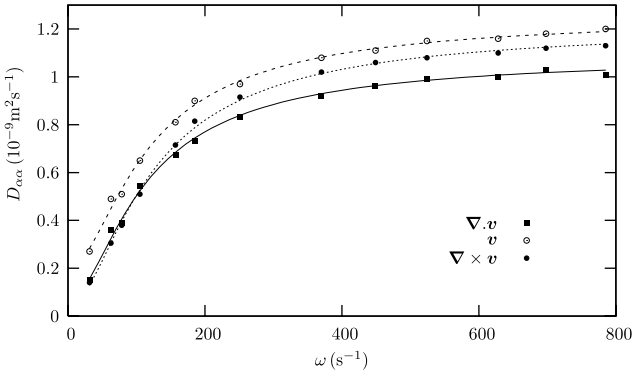

Fig. 7. Diffusion spectrum of an onion phase: diffusion is measured along the flow-gradient ($\vec{\nabla}\vec{v}$), flow ($\vec{v}$), and vorticity ($\vec{\nabla}\times\vec{v}$) directions. The solid lines represent fitting of the data with Eq. (8). Note that error bars in the measured diffusion coefficients are on the order of 1–2%, the size of the data points.

experimental conditions [15]. The corresponding experimental results are displayed in Fig. 7. Significant discrepancies are observable between the three encoding directions. In particular, for the high-frequency region of the spectrum ($\frac{2\pi}{\tau_c} \gg \omega \gg \frac{2\pi}{\tau_d}$), solvent diffusion can approximately be written, following Eq. (6):

$$\langle D_{\alpha\alpha}\rangle = \tfrac{1}{3}D_{\mathrm{perm}} + \tfrac{2}{3}D \tag{9}$$

Parameters obtained by fitting the diffusion spectra shown in Fig. 7 are D_{perm}, D and R. D_{perm} particularly affects the spectrum at low frequencies, D particularly affects the spectrum at high frequencies, and R affects the "turnover frequency", in other words, the shape of the spectrum. However in the case of the radius, the primary quantity measured is a time constant and this is turned into a radius via a knowledge of D.

Discrepancies between the three directions at high frequencies seem therefore to indicate that there exist differences in permeation coefficients in the three directions. The remaining discrepancy in the shape of the spectra must arise from different apparent onion radii and hence vesicle deformation. For the $\vec{\nabla}\vec{v}$ direction, fitting of the experimental data with Eq. (8), we set: $D = 1.6\times10^{-9}\ m^2\ s^{-1}$, in agreement with numerical values obtained experimentally for solvent diffusion along the lamellae at low shear rates. The corresponding vesicle radius is found to be:$R_{\vec{\nabla}\vec{v}} = 6.9\ \mu m$. For the $\vec{v}$ and $\vec{\nabla}\times\vec{v}$ directions, we accommodate for deviations from the ideal spherical topology by letting D take values $D_{\vec{v}}$ and $D_{\vec{\nabla}\times\vec{v}}$, respectively, thereby altering the values of $R_{\vec{v}}$ and $R_{\vec{\nabla}\times\vec{v}}$ obtained. These deviations are recovered using the radial direction as a reference according to (see Eq. (8):

$$R_{\vec{v},\vec{\nabla}\times\vec{v}} = R_{\vec{\nabla}\vec{v}} \times \sqrt{\frac{D_{\vec{v},\vec{\nabla}\times\vec{v}}}{1.6\times10^{-9}\ \mathrm{m^2\ s^{-1}}}} \tag{10}$$

The fitting of the experimental data leads to (see Table 1): $D_{\vec{v}} = 1.78\times10^{-9}\ m\ s^{-1}$ and $D_{\vec{\nabla}\times\vec{v}} = 1.8\times10^{-9}\ m\ s^{-1}$, leading to: $R_{\vec{v}} \approx R_{\vec{\nabla}\times\vec{v}} \approx 7.3\ \mu m$, thus indicating that the vesicles might be slightly flattened along the $\vec{\nabla}\vec{v}$ direction, consistent with previous suggestions [21,25], although the effect is within the range of our error estimates. Hence we make no assertion here of significant deviation from spherical shape.

Note the value of the permeation coefficient along the flow direction: $D_{\mathrm{perm}} \approx 2\times10^{-10}\ m^2\ s^{-1}$, considerably higher than for the two other directions. Under the longest

Table 1
Characteristics of the shear-induced vesicles obtained by fitting of the experimental diffusion spectra with Eq. (8)

	D_{perm} ($\times10^{-10}$ m^2 s^{-1})	R (μm)
$\vec{\nabla}\vec{v}$	0.7 ± 0.2	6.9 ± 0.2
$\vec{v}$	2 ± 0.2	7.3 ± 0.2
$\vec{\nabla}\times\vec{v}$	0.4 ± 0.2	7.3 ± 0.2

Here we set $D = 1.6\times10^{-9}\ m^2\ s^{-1}$ in agreement with our measurement of solvent diffusion parallel to the membranes, at shear rates below onion formation.

duration accessible in our experiments ($T = 200$ ms), the average distance traveled through the onions is therefore ≈ 9 μm, on the order of the onion size. Probing by the spins of different onions over the experimental time may therefore be of importance and should be accounted for in a complete description of solvent motion. However, these considerations are only relevant for the lowest accessible frequencies. Moreover, since $D_\perp \leqslant 0.1 D_\parallel$, in the time taken to diffuse around the MLVs, the squared radial distance permeated is $\leqslant 0.1 r^2$. Hence, very little effect on τ_d is expected ($\tau \sim \frac{r^2}{D}$). It should also be noticed that the diffusion data presented here suggest that water molecules outside the onions contribute little to the signal. In particular, the very slow diffusion observed at long frequencies, consistent with the permeation value, suggests that there does not exist a significant fraction of water outside the onions and free to diffusive over long distances. Despite the simple assumptions underlying our theoretical model, the agreement between the experimental data and the fits obtained from Eq. (8) is very satisfactory.

5. Conclusion

The formation of multilamellar vesicles has been shown with the vesicle size measured by diffusion spectrum NMR, based on a simple phenomenological model to account for the effect of the onions on solvent diffusion. Solvent permeation is found considerably faster along the flow direction. A larger interlayer spacing or a greater number of defects along this direction may be explanations for this fact. We believe that the multiple gradient pulse NMR method which we have used provides an effective tool for measuring onion size under shear. A detailed study of shear-dependent onion size will be the subject of a future article.

References

[1] G.T. Barnes, I.R. Gentle, An introduction to interfacial science, Oxford University Press, 2005.
[2] K. Holmberg, B. Jönsson, B. Kronberg, B. Lindman, Surfactants and polymers in aqueous solution, John Wiley & sons Ltd, 2003.
[3] D.F. Evans, H. Wennerström, The colloidal domain, Wiley-vch, 1999.
[4] R.G. Larson, P.T. Mather, Theoretical Challenges in the dynamics of complex fluids, T.C.B. McLeish Kluwer Academic Publishers, Dordrecht, 1997.
[5] R.G. Horn, M. Kléman, Ann. Phys. 3 (1973) 229.
[6] J.N. Israelachvili, Intermolecular and surface forces, Academic Press, 1985.
[7] W. Helfrich, Z. Naturforsch. 33a (1978) 305.
[8] C.R. Safinya, D. Roux, G.S. Smith, S.K. Sinha, P. Dimon, N.A. Clark, A.M. Bellocq, Phys. Rev. Lett. 57 (1986) 21.
[9] S. Leibler, R. Lipowsky, Phys. Rev. B 35 (13) (1987) 7004–7009.
[10] A. Al Kahwaji, O. Greffier, A. Leon, J. Rouch, H. Kellay, 1 Phys. Rev. E 63 (2001) 041502 .
[11] M. Imai, K. Nakaya, T. Kato, Euro. Phys. J.E 5 (2001) 391.
[12] S. Muller, C. Borschig, W. Gronski, C. Schmidt, D. Roux, Langmuir 15 (1999) 7558.
[13] M. Lukaschek, S. Muller, A. Hansenhindl, D.A. Grabowski, C. Schmidt, Colloid Polym. Sci. 274 (1996) 1.
[14] A. Lutti, P.T. Callaghan, Phys. Rev. E 73 (2006) 1.
[15] A. Lutti, P.T. Callaghan, Jour. Magn. Res. 180 (2006) 83–92.
[16] A.G. Zilman, R. Granek, Eur. Phys. J. B (1999) 593–608.
[17] A. Leon, D. Bonn, J. Meunier, A. Al-Kahwaji, O. Greffier, H. Kellay, Phys. Rev. Lett. 84 (6) (2000) 1335–1338.
[18] L. Courbin, J.P. Delville, J. Rouch, P. Panizza, Phys. Rev. Lett. 89 (2002) 148305.
[19] O. Diat, D. Roux, F. Nallet, Phys. Rev. E 51 (4) (1995) 3296.
[20] J.B. Salmon, S. Manneville, A. Colin, Phys. Rev. E 68 (2003) 051503.
[21] O. Diat, D. Roux, F. Nallet, J. Phys. II, France 3 (1993) 1427–1452.
[22] H.Y. Carr, E.M. Purcell, Phys. Rev. 94 (3) (1954) 630–638.
[23] S. Meiboom, D. Gill, Rev. Sci. Instrum. 29 (8) (1958) 688–691.
[24] S. Meiboom, Z. Luz, D. Gill, Journ. Chem. Phys. 27 (6) (1957) 1411–1412.
[25] J. Zipfel, F. Netteshem, P. Lindner, T.D. Le, U. Olsson, W. Richtering, Europhys. Lett. 53 (2001) 335.
[26] J. Stepisnik, Physica B 104 (1981) 350–364.
[27] P.T. Callaghan, J. Stepisnik, Adv. Mag. Opt. Res. 19 (1996) 325.
[28] P.T. Callaghan, J. Stepisnik, Jour. Magn. Res., Series A 117 (1995) 118–122.
[29] J. Stepisnik, P.T. Callaghan, Magn. Reson. Imaging 19 (2001) 469–472.
[30] J. Stepisnik, A. Mohoric, Duh A. 307 (2001) 158–168.
[31] P.T. Callaghan, S.L. Codd, Phys. Fluids 13 (2) (2001) 421–427.
[32] P. Hervé, D. Roux, A.-M. Bellocq, F. Nallet, T. Gulik-Krzywicki, J. Phys. II, France 3 (1993) 1255–1270.